ELSEVIER

Thermochimica Acta 316 (1998) 47–56

thermochimica acta

Frequency domain calorimetry to study phase transitions and relaxation processes in condensed matter

G. Salvetti*, C. Ferrari, E. Tombari

IFAM-CNR,via del Giardino 7, 56127 Pisa, Italy

Received 11 September 1997; received in revised form 7 February 1998; accepted 9 February 1998

Abstract

This paper describes a modulated scanning calorimeter for studying, both in the isothermal and in the temperature scanning mode, liquids and solids that are chemically stable or undergoing structural transformations. The calorimeter concurrently measures, at a temperature modulation frequency, the complex heat capacity C_p^* and the enthalpy change during chemical reactions or phase transitions. The time and temperature variation of the real and the imaginary parts of C_p^* provide information on the molecular relaxation processes and the mutual influence between structure and dynamics in highly viscous samples as well as the glass transition. The principles and main features of the instrument and a set of experimental tests performed are described and accuracy, sensitivity, temporal stability and reproducibility of the data are given. © 1998 Elsevier Science B.V.

Keywords: Glass transition; Heat capacity; Temperature modulated DSC

1. Introduction

The frequency-dependent heat capacity is being measured for several decades, but a study by Birge and Nagel [1] gave the technique a stimulus for further development and wider application. These applications not only include the investigations of slow molecular dynamics, mainly configurational, but also the glass⇄liquid transition, owing to its dynamic nature.

The quantity to be measured in these systems is analogous to a complex susceptibility. It relates the heat supplied to the temperature of the sample, in close analogy with the dielectric susceptibility which relates the electric field to polarisation. In this sense, frequency domain calorimetry (FDC) results are complementary to dielectrometry [2], although the relaxation processes probed in the two techniques differ: the dipole rotational relaxation is observed by dielectrometry, while all the hydrodynamic processes active in the sample (the rotational one included) are observed by FDC.

A variety of commercial devices have now become available; their functions and applications have been reviewed recently and benefits and problems related to their use given [3–5]. Before the availability of such equipment, a technique and an instrument was developed for measuring the average heat capacity of a material during the course of its chemical reactions and phase transformations. They were applied to the study of polymerisation kinetics [6,7]. More recently,

*Corresponding author. Tel.: (+39) 50 31 39 020; fax: (+39) 50 31 39 035; e-mail: salvetti@ifam.pi.cnr.it

PII S0040-6031(98)00303-7

the technique was used to study the complex heat capacity C_p^* and, through it, the nature of the changing of molecular dynamics in an isothermal condition [8]. This was an advance over the Birge and Nagel method [1], which is unsuitable for polymer studies.

As part of continuing attempts at measuring thermodynamic and molecular dynamic behaviours of materials undergoing a chemical and physical transformation, a simultaneous impedance and thermal analyser (SITA) was developed, which was used for correlating the thermodynamics of transformation with dielectric relaxation and dc conductivity [9]. In this paper, a further advance on the earlier instrumentation is reported [8]. This allows the determination of not only the complex C_p^*, in both isothermal and temperature scanning mode, but also the enthalpy, ΔH, of the chemical and physical transformations occurring over time scales of several days as required for studies on biopolymers.

The paper is organised as follows:

(i) the description of the calorimeter;
(ii) the operational principle, the theory and the procedure for calculating real and imaginary parts of C_p^* and ΔH;
(iii) the experiments performed to obtain the accuracy, sensitivity and the time stability of the instrument; and
(iv) results of several studies.

2. Experimental details

2.1. The calorimetric cell

Modulated scanning calorimeter, MSC, is a modification of an isothermally operating instrument developed for the simultaneous measurements of C_p^* and ΔH of materials undergoing chemico-physical transformations [10]. The calorimetric head of that instrument has been retained, while the calorimetric cells and their operation have been modified.

In Fig. 1, the vertical section of the sample cell and the walls of the cylindrical hole, drilled in the calorimetric head, in which the cell is located, are shown. The walls are at the temperature T_B of the calorimetric head, which acts as the thermal bath for the heat flow from the cell. Two wires were uniformly wound on the

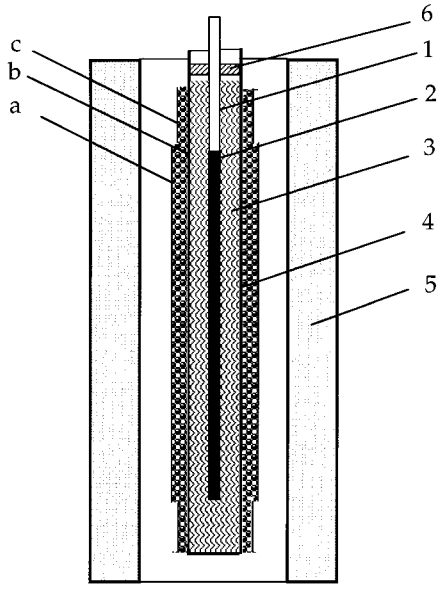

Fig. 1. The schematic vertical section of the sample cell: 1, Pyrex capillary tube; 2, sample; 3, mercury; 4, stainless-steel tube; 5, massive aluminium walls; 6, Teflon plug (a second plug is on the top of the cell); a, b, c , the absolute temperature sensor, the differential temperature sensor and the heater, respectively.

surface of the final part (l=100 mm) of a stainless-steel capillary tube (L=400 mm; o.d.=5 mm; i.d.=4.6 mm) which constitutes the cell: one is a heater made with manganin wire and the others are two sensors made with type 99 nickel alloy wires (o.d.=0.05 mm) of high temperature coefficient, produced by Driver-Harris. A second sensor was wound in such way as to exclude the top and the bottom of the cell (see Fig. 1, part a), where most of the axial temperature gradients are localised. The sample was positioned in the corresponding region of the cell, so the sensor gives the mean temperature value of the sample. The sample container is a Pyrex precision capillary tube (o.d.=2.2 mm; i.d.=1.6 mm; l=130 mm), which, in a typical experiment, is weighed, filled with the sample, sealed by flame, weighed again and then positioned on the axis of the cell by a holder. The sample holder was made with a stainless-steel capillary tube, sufficiently long to obtain both, a low thermal coupling and easy access to the sample from outside. The reference cell is identical to the sample cell, except for a second

manganin wire heater, which was wound in the same place as the outer sensor of the sample cell (see Fig. 1). The cells were filled, up to the heater height, with mercury to obtain a good thermal coupling among heater and sensor wires and the sample. In these conditions, the heat-diffusion characteristic time inside the cell was only a few seconds, while the characteristic time between the cell and the thermal bath was ca. 200 s. Convection currents around the cell walls were prevented owing to the small radial distance from the thermal bath (<2 mm). Safety problems, relating to the use of mercury, have been solved with the use of long cells of small diameter, sealed with two Teflon caps which also support the sample holder on the axis of the cell: one near the free surface of mercury, the other at the top of the cell. The sample must be introduced when the cell is at room temperature, that is when the mercury vapour pressure is ca. 10^{-6} bar.

The use of anti-adhesive products prevents the formation of small spheres of mercury on the surface of the glass capillary tubes containing the sample, hence reducing the risk of mercury dispersion in the laboratory.

2.2. Experimental setup

Fig. 2 shows the block-diagram of the experimental setup of the calorimeter, obtained by assembling commercial instruments of general use in research laboratories. To scan and modulate the sample temperature, the software LabVIEW by National Instruments was installed and a suitable program created. It changes the temperature set point according to the program, compares the real temperature of the sample with the set point value and, through the proportional, integral and derivative (PID) actions of a control procedure, changes the power supplied to the cell heater to track the programmed temperature profile. The reference cell heater was electrically connected in parallel to the sample cell heater to minimise the effect of the programmable power supply (PPS1) instability, and to obtain its temperature evolution such as the one for the sample cell. The sample temperature, T_S, is calculated from the value of the outer sensor resistance, which is measured with a programmable multimeter HP Model 34401A.

A cold source on the cells was not foreseen, so it is impossible to scan the cell temperature below that of

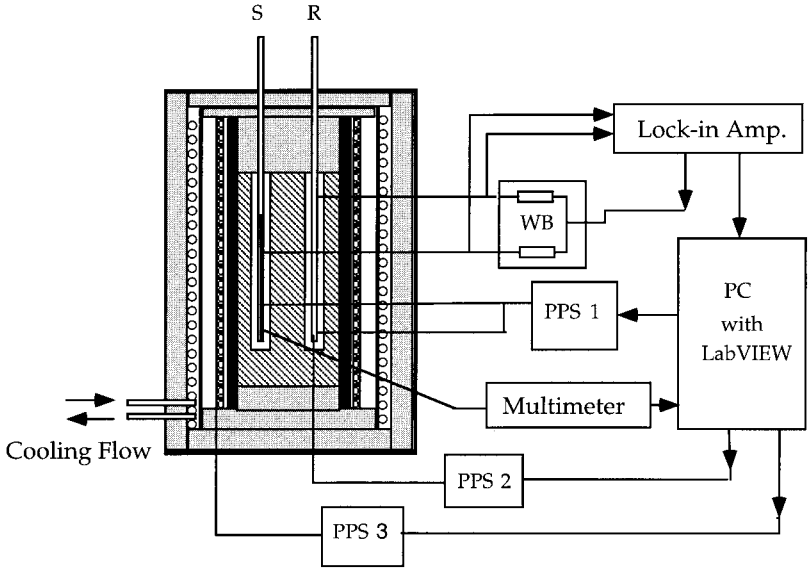

Fig. 2. The block-diagram of the calorimeter: S, the sample cell; R, the reference cell; PC, IBM 486 personal computer; WB, Wheatstone bridge; PPS1, PPS2, PPS3, programmable power suppliers; and Multimeter, HP 34401A or an equivalent one. The lock-in amplifier may be the Stanford SR510 or SR830 or an equivalent one The cooling flow is maintained at 253±0.5 K.

the bath, and to modulate it. The modulation facility can be gained by setting T_S a few degrees above the bath temperature T_B (typically $T_S=T_B+10$ K). If the two twin-cells contain equal and empty glass capillary tubes, during the temperature scanning the reference cell temperature, T_R, would remain equal to T_S. When one tube is filled with the sample material and if exothermic or endothermic processes occur in it, the enthalpy release rate, dH/dt, is a power which adds to the power supplied to the sample cell to attain the programmed temperature. Consequently, the PID controller reduces the power by the same amount, hence reducing the temperature of the reference cell. In this way, thermal events occurring in the sample cell are reflected on the reference cell temperature.

To maintain T_R equal to T_S, a second PID control procedure, included in the software, drives the PPS2 which feeds with a power, $P_R(t)$, the second heater of the reference cell to nullify the output of the Wheatstone bridge, WB, as seen in Fig. 2. The sensor of the sample cell (see in Fig. 1) and the corresponding one of the reference cell are connected to WB, which also includes two equal low-temperature coefficient resistors. It is fed with the output signal of the internal oscillator of the lock-in amplifier, which operates in the internal mode and at the frequency of 87 Hz to measure, with high sensitivity, the WB voltage output.

The power $P_R(t)$ contains all information necessary to characterise the sample thermodynamically. Indeed, $P_R(t)$, for fixed values of the modulation amplitude and frequency, depends on: the complex heat capacity of the sample, the enthalpy release and the temperature scan rate. The sensitivity of the calorimeter is related to the sensitivity of the lock-in amplifier, and can be increased by increasing the temperature modulation amplitude. The PC software also stores the data of interest: the sample temperature, the T_R-T_S value, i.e. the lock-in amplifier output, and $P_R(t)$. The analysis program uses these data to calculate the absolute values of the change in enthalpy and the real and imaginary parts of the complex heat capacity of the sample.

3. Theory and measurement principle

3.1. The heat flow equations

The heat flow from the calorimetric cell in Fig. 1 can be analytically described by a set of differential equations [11], under the assumption of a cylindrical symmetry and of negligible axial heat exchange from the cell for which the length-to-diameter ratio is ≥ 20. As the heat diffusion inside the cell occurs over a very small time compared with the modulation period, the temperature T_S of the cell is, to a good approximation, equal to the temperature of the sample. In these experimental conditions and until the above assumptions are verified, the heat balance equation of the cell is,

$$dH_x(t,T_S)/dt + C_S dT_S/dt + K_S(T_S,T_B) = P_S(t,T_S) \quad (1)$$

where the first term of the left-hand side is the enthalpy-change rate, also containing the contributions coming from the physico-chemical processes occurring in the sample, C_S the heat capacity of the empty cell, the power flow, K_S , from the cell being an instrumental function depending on the geometry and the materials of the calorimetric head, and $P_S(t)$ the power supplied to the cell heater.

The corresponding equation for the empty reference cell is,

$$C_R dT_R/dt + K_R(T_R,T_B) = P_R(t,T_R) + P_B(t,T_R) \quad (2)$$

$P_B(t, T_S)$ is the power supplied to the reference cell throughout the second independent heater.

The measuring procedure is based on the attainment of the following conditions:

$$C_S = C_R;\ K_S = K_R \quad (3a)$$

$$P_S(t) = P_R(t) \quad (3b)$$

$$T_R(t) - T_S(t) = \Delta \quad (3c)$$

$$T_S(t) = T_1 + \beta t + T_m \cos \omega t \quad (3d)$$

where Δ is a constant, T_1 the initial temperature, β the temperature scanning rate, and T_m the temperature modulation amplitude.

The first condition is achieved by building two twin-cells, positioned on the axis of two identical cylindrical holes, drilled in the massive calorimeter head. When operating in the differential operation mode, the twin-cells condition allows us to subtract from the calorimeter signal all the spurious contributions, affecting both the sample and the reference cell. In this way, the signal-to-noise ratio is highly increased. The differential condition is obtained by connecting

the thermal resistors (the sensors) of the two cells in a Wheatstone bridge. The off-balance δV of the bridge is related to the temperature difference between the two cells, δT, by the equation

$$\delta V/V = S(T_S)\delta T \quad (4)$$

where V is voltage signal applied to the bridge, and $S(T_S)$ a function including the thermal coefficient of the sensors, which is either known or calculated after a suitable calibration procedure. When no power is supplied to the cell heaters, $T_S=T_R=T_B$, that is $\delta T=0$. If $\delta V\neq 0$, it can be set at zero by activating a small variable resistor, connected in one of the arms in order to balance the bridge. One would expect $\delta V=0$, also when the same power was supplied to the two cells. In practice, the δV signal is very small, owing to small unavoidable differences between the cells and the heat exchange coefficients.

To achieve condition (3c) it is sufficient to induce an offset, δV_0, by activating the balance resistor, so that

$$\delta V_0 = VS(T_S)\Delta \quad (5)$$

and to turn on the PID control procedure, which regulates the power, P_B, supplied to the second independent heater of the reference cell. If the PID setting point is $\delta V=0$, the controller increases the power until the balance of the WB is again attained.

The last condition is achieved by the PID controller acting on the power supplied to the cells electrically in parallel to accomplish condition (3b). If the PID set point is changed following the function in (3d), the sample cell temperature, measured by the outer sensor (see Fig. 1), tracks the desired temperature profile, while the reference cell temperature changes at the same rate, maintaining itself at Δ above the sample temperature.

In an ideal instrument, when the sample cell is empty and the quantities in (3a) are temperature independent, $P_B(t,T_S)$ would be equal to the constant value, P_0, necessary to maintain the Δ difference. In practice $P_0(t,T_S)$ is stored as a function of time and temperature, which represents the operative baseline of the calorimeter.

In summary, the calorimeter measures the power, $P_B(t,T_S)$, necessary to maintain the reference cell at Δ degrees above the sample cell, while it follows the programmed temperature profile $T_S(t)$. A preliminary run, with the empty sample cell, gives $P_0(t,T_S)$. These two functions contain all the information necessary to characterise the sample, as can be easily seen by subtracting Eq. (2) from Eq. (1), which yields,

$$P_B(t,T_S) - P_0(t,T_S) = -dH(t,T_S)/dt \quad (6)$$

Data analysis gives the in-phase and the out-of-phase components of the signal, at the modulation frequency, ω, during the experimental run. These components assume different meanings, according to the processes occurring in the sample. The typical cases are:

(i) A glass transition occurs in the sample. The enthalpy change rate reflects the structural relaxation processes and the two components give the real and the imaginary parts of the complex heat capacity, related by the Kronig–Kramers equations [12];
(ii) The sample structure changes in time and/or owing to the temperature change, but the thermodynamic equilibrium at the modulation frequency is maintained. The out-of-phase component is always equal to zero and the in-phase component gives the heat capacity as a function of the sample structure; and
(iii) The sample undergoes a first-order phase transition; it is at a thermodynamic equilibrium and the temperature modulation affects the transition kinetics. The result is the appearance of an out-of-phase component, while the in-phase component maintains the usual meaning. The modulated calorimetry data contains also information on the kinetics of the process occurring in the sample if a theory of the process is available [13–15].

3.2. Signal processing

Recently, with the increasing interest in modulated calorimetry, many theoretical models for analysing the experimental curves have been developed and published [16,17]. The mathematical model of the calorimetry described in this paper is based on the possibility of describing, to a very good approximation, the heat flow from the cell owing to its cylindrical symmetry and the features reported here, which were previously patented [18,19].

Let us now consider Eq. (6) and the temperature profile in Eq. (3d) in order to relate the measured

$P_B(t,T_S)$ to the thermodynamic quantities. If a sinusoidal modulation, $\Delta T=T_m \cos \omega t$, is imposed on the sample and a linear response behaviour is assumed, the sample enthalpy change oscillates at the same frequency ω, but with a phase difference ϕ relative to the temperature, that is

$$\Delta H = H_m \cos(\omega t + \phi) \tag{7}$$

ΔH can be split in two oscillating terms: one in-phase and the other out-of-phase with the temperature

$$\Delta H = C'_x T_m \cos \omega t + C''_x T_m \sin \omega t \tag{8}$$

where $C'_x = H_m \cos \phi / T_m$ and, $C''_x = H_m \sin \phi / T_m$

The rate of enthalpy variation due to the modulation of temperature can be derived from Eq. (8).

$$dH/dt = -\omega C'_x T_m \sin \omega t + \omega C''_x T_m \cos \omega t \tag{9}$$

The contribution from the slow linear change of the temperature is given by the well-known relation applied in scanning calorimetry

$$dH/dt = C_x \beta \tag{10}$$

where C_x is the equilibrium heat capacity of the sample; it is equal to C'_x when the sample is in thermodynamic equilibrium at the modulation frequency.

When the temperature variation (see Eq. (3d)) is sufficiently slow, the endo/exothermic contributions to the rate of enthalpy change, due to chemical or physical processes occurring in the sample, are, to a good approximation, only time-dependent, that is

$$dH/dt = \partial H/\partial t \tag{11}$$

Summing all the contributions in Eqs. (9)–(11), one obtains the total enthalpy variation rate, and Eq. (6) becomes

$$P_B(t,T_S) - P_0(t,T_S) = -\partial H/\partial t - C_x \beta + \omega C'_x T_m \sin(\omega t) - \omega C''_x T_m \cos(\omega t) \tag{12}$$

From the analysis of the power difference supplied in the time interval $n\tau<t<(n+1)\tau$ in terms of the discrete Fourier transform at the frequency ω, with the following assumptions: (i) the enthalpy release rate $\partial H/\partial t$ is, according to a Taylor expansion, limited to the first-order term; and (ii) the heat capacity components are time-invariant during τ, one obtains

$$P_x(t,T_S) - P_0(t,T_S) \cong \overline{P}_n + P' \cos(\omega t) + P'' \sin(\omega t) \tag{13}$$

where $\overline{P}_n$ is the average power value, P' and P'' are the in-phase and out-of-phase components, respectively. From Eqs. (12) and (13), the following relations for the measured thermodynamic quantities of interest are deduced:

$$(\partial H/\partial t + C_x \beta)_{t=n\tau} = -\overline{P}_n \tag{14a}$$

$$C'_x(\omega, t = n\tau) = \frac{1}{\omega T_m}(P''_n - (\overline{P}_{n+1} - \overline{P}_n)/\pi) \tag{14b}$$

$$C''_x(\omega, t = n\tau) = -\frac{P'_n}{\omega T_m} \tag{14c}$$

In principle, these relations should give the absolute values of C'_x, C''_x and $\partial H/\partial t$. In practice, a few instrumental spurious effects must be taken into account. The more important ones are:

(i) the time delay introduced by the PID controllers;
(ii) the time delay due to the diffusion of heat from the heaters to the sample; and
(iii) the temperature gradients along the sample cell.

It has been verified that, in order to remove these effects, it is sufficient to introduce a scaling factor and a phase shift in the measured $P_B(t,T_S)$. Alternatively, one can utilise a reference material, whose heat capacity is known in the temperature interval of interest, to determine the instrumental function.

In conclusion, to obtain the absolute value of the heat capacity in an easy and reliable way, two preliminary runs are necessary: the first without the sample, the second with a reference material.

4. Chemicals

The experimental samples were prepared with commercial products utilised without further purification. The nominal purity and the producer of each substance were: diglycidyl ether of bisphenol-A (DGEBA) – purity unknown, obtained as EPON 828EL from Shell Company; dodecane – 99%, from Fluka; cyclohexylamine – 99%, from Aldrich; ethylene glycol – 99%, from Baker; glycerol – anhydrous 99.5%, from Fluka; mercury – 99.5%, from Carlo Erba; and water – bidistilled, from Angelini.

5. Instrument tests

The differential operation mode and the adopted measuring procedure allow the absolute value of $C'_p(\omega)$, $C''_p(\omega)$ and $\partial H/\partial t$ of a sample to be calculated, from Eqs. (14a),(14b) and (14c). To put the calorimeter to test, the following were measured:

(i) the calorimeter base-line stability, with the two cells containing empty capillaries;
(ii) $C'_p(\omega)$ and $C''_p(\omega)$ of few materials at 298.1 K; and
(iii) the $C'_p(\omega)$ and $C''_p(\omega)$ against the temperature of mercury and dodecane between 298 and 383 K, using ethylene glycol as the reference material.

The results of the tests (i) and (iii) are shown in Fig. 3 and 4, respectively.

The base-line stability for $C'_p(\omega, T)$ and $C''_p(\omega, T)$ was high, while for $\partial H/\partial t$ the stability was limited by the slow oscillations of the room temperature, which affect the lock-in amplifier and the WB.

For validation, the measured $C'_p(\omega, T)$ values must be in good agreement with the data from standard calorimetric methods, while $C''_p(\omega, T)$ must be zero, these materials being in thermodynamic equilibrium at the temperatures and frequency of the experiments. These features, particularly $C''_p(\omega, T) = 0$, were difficult to attain, until recently, with commercial calorimeters and this quantity is generally not reported in published papers [21]. The measured molar heat capacity of water, dodecane, mercury and glycerol at 298.1 K agreed within 1% with the values reported in literature [22–25]; the same agreement was

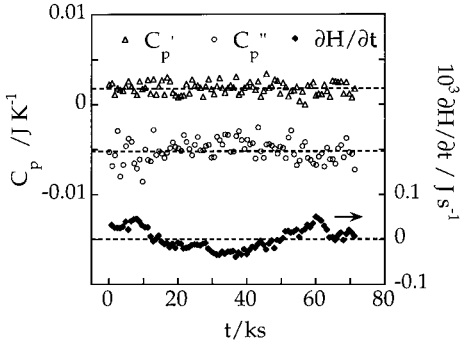

Fig. 3. Plots of C'_p, C''_p and $\partial H/\partial t$ vs. time, to test the stability and sensitivity: the sample cell was empty and the fluctuation of the room temperature over 24 h was within ±2 K.

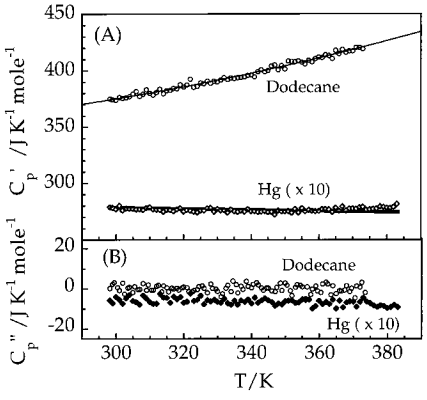

Fig. 4. Plots of C'_p and C''_p vs. temperature of mercury and dodecane: the reference material was ethylene glycol [20]; mercury data from Ref. [24] have been fitted to the straight line drawn on our experimental points. The measured C'_p values of dodecane from 293 to 370 K have been fitted to the equation: $C'_p(T) = 394.74 - 0.62134T + 0.001854T^2$.

obtained for the molar heat capacity of mercury against temperature, while the comparison was not possible for dodecane since the corresponding data was not found in literature. So the heat capacity values of dodecane between 298 and 383 K reported here, represent the first experimental determination rather than a test. The values of $C''_p(\omega, T)$ are affected by a systematic error due to the finite thermal conductivity of the sample, which introduces a time delay in the measured power. Anyway, the effect is small and within ±0.008 J/K.

To evaluate the sensitivity and the accuracy of the calorimeter, the statistical nature of the data set, collected at a rate of $\omega/2\pi$ points per second, must be considered. The true value of the measured quantity is the mean, and the standard deviation of the mean is seen as the precision of the measurement. Precision is generally an upper limit to accuracy owing to possible systematic errors. Sensitivity, as the capability of the calorimeter to observe the minimum change of the measured quantity, as well as time stability are important in applications concerning slow processes such as the physical ageing of the amorphous solids.

In this instrument, the sensitivities of C'_p and C''_p measurements were limited by the temporal stability, i.e. by the residual slow oscillations of the data smoothing curve, as for example around the ideal horizontal straight line, expected when the sample

is chemically stable and the measurement is performed at constant temperature (see Fig. 3). This accuracy is related to the accuracy of the measured $P_B(t,T_S)$. The accuracy of $\partial H/\partial t$ values was strongly limited by the long-period instability of the lock-in amplifier and of the WB, due to the day- and-night oscillation of room temperature. Consequently, the accuracy and sensitivity depend on the measurement duration.

To test the data reproducibility, four independent measurements were performed with different samples of mercury during a time period of four months, while changing the modulation frequency and/or the modulation amplitude. The scattering of the data around the mean value was within ±0.003 J/K.

The main features of the calorimeter are the following:

(a) *base-line stability* (per day and per K of room temperature variation) vs. time and at constant sample temperature: $\partial H/\partial t \pm 50\ \mu W$; $C'_p(\omega) \pm 0.002$ J/K; $C''_p(\omega) \pm 0.002$ J/K;
(b) *accuracy*: $\partial H/\partial t \pm 50\ \mu W$; $C'_p(\omega) \pm 0.001$ J/K; $C''_p(\omega) \pm 0.001$ J/K; $T_S \pm 0.1$ K;
(c) *sensitivity*: $\partial H/\partial t \pm 1\ \mu W$; $C'_p(\omega) \pm 0.0002$ J/K; $C''_x(\omega) \pm 0.0002$ J/K; $T_S \pm 0.0003$ K; these values are the average of 100 data points stored in one modulation period.
(d) *temperature gradients in the sample* (with $T_S - T_B = 100$ K): 0.1 K.

The gradients are localised at the ends of the sample; their values decrease about linearly with $T_S - T_B$ value.

6. Calorimetric performance

To outline the performance of the calorimeter, we studied the curing process of a thermosetting polymer DGEBA+cyclohexylammine (1 : 1 in moles) at 298.1 K, up to the sample vitrification. After vitrification, the chemical reaction rate in the sample practically reduces to zero under diffusion control; increasing the sample temperature increases the sample dynamics and glass-softening occurs. In these conditions, the chemical reaction starts again and new bonds are created, producing an effect on the sample dynamics, which is competitive with the temperature increase. Anyway, if the upper temperature attained during the scanning run is sufficiently high, the sample remains in the supercooled liquid state (relative to the measuring frequency). During a sufficiently long storage at that temperature, the chemical reactions stop under mass control. When the temperature is scanned downwards, the sample dynamics is increasingly slowed, until the characteristic relaxation times of the internal modes again become comparable to the modulation period. The sample undergoes the temperature-induced glass transition as displayed by the sigmoidal shape of C'_p curve and the corresponding peak in the C''_p curve. At the end of the run, the sample attains the initial curing temperature, but it is now chemically stable and the occurrence of physical ageing changes its structure in the time scale of the sample dynamics at the storage temperature.

The vitrification at constant temperature, glass-softening, increase in the structure complexity until a new glass transition occurs, owing to the increase of the number of bonds on heating, and the glass transition

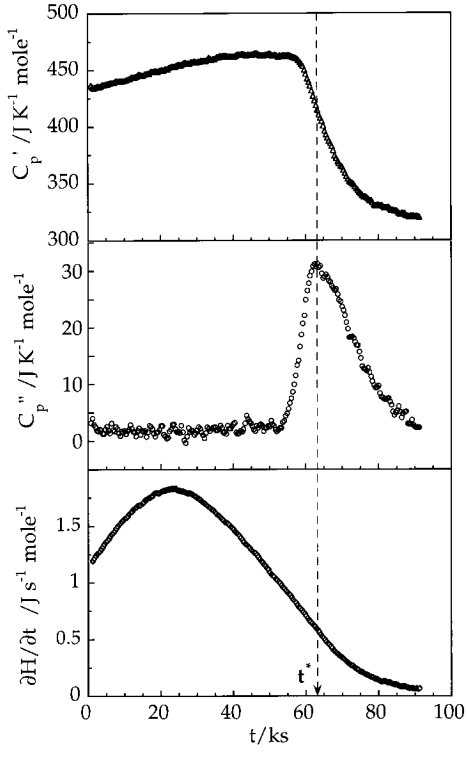

Fig. 5. The C'_p, C''_p and $\partial H/\partial t$ of DGBA+cyclohexylamine (1 : 1 in moles) at 298.1 K: t^* marks mixture vitrification at the modulation frequency of 5 mHz.

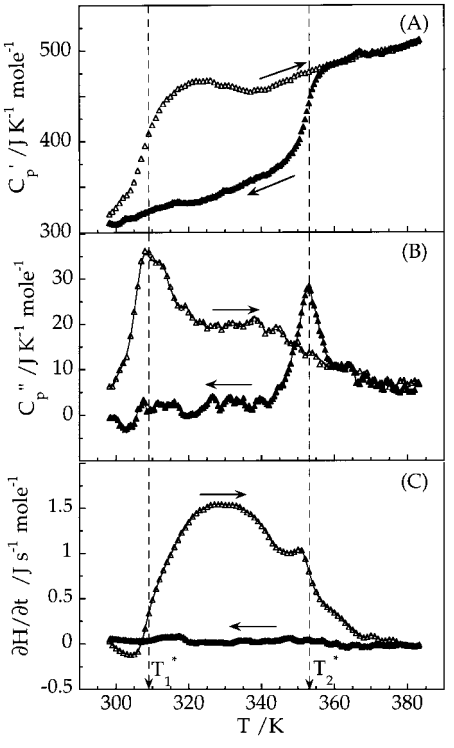

Fig. 6. Plots of C'_p, C''_p and $\partial H/\partial t$ vs. temperature, scanning up and down in temperature the sample after curing at 298.1 K for ca. 1 day, as determined in Fig. 5: T_1 and T_2 mark the glass-softening and glass transition, respectively, at the modulation frequency of 5 mHz; the temperature scanning rate and the modulation amplitude were 0.06 K/min, 0.25 K, respectively.

on cooling, as reflected on C'_p, C''_p and $\partial H/\partial t$ curves, are shown in Fig. 5 and 6. Subtle effects associated with the enthalpy recovery have also been detected by this calorimetry, but excluded from this paper in the interest of its limited scope. An application of modulated scanning calorimetry to the study of the cure, vitrification and devitrification of thermosetting systems has been recently published [26]. The reported results are qualitatively comparable with those in Fig. 6, even if the imaginary part of the heat capacity was not measured. It is necessary to stress that the identification of the vitrification and the glass transition is reliable only in presence of the simultaneous occurrence of the peak in C''_p curve and the sigmoidal shape of the C'_p curve. Moreover, C''_p vs. C'_p data can be analysed to obtain quantitative information about the relaxation process [1,7]. The relevance of a simultaneous measurement of C'_p, C''_p and $\partial H/\partial t$ has also been proved in the characterisation of diepoxide-diamine compositions which show a two-stage-network growth [27].

7. Conclusions

The aim of this paper was to report the detailed description of a modulated scanning calorimeter, based on an original design of the calorimetric cell, and its performances. The tests performed on liquid samples have shown high sensitivity, good accuracy and the ease of the procedure for the absolute measurement, both in isothermal mode and in the temperature scanning mode. This calorimeter is a further instrumental solution for modulated calorimetry, allowing the simultaneous measurement of $C'_p(\omega, T)$, $C''_p(\omega, T)$ and $\partial H/\partial t$ with high sensitivity and accuracy. An important feature is its adaptability to match the requirements of an experiment, it being possible to change widely the cell dimensions (only the length/diameter ratio must be maintained) and the sample conditions in the cell (pressure, humidity, possibility of photo-activation, etc.). To show the quality of the calorimetric data, the characterisation of a sample undergoing structural transformations, due to polymerisation and dynamic processes as vitrification and glass transition, is also reported.

Acknowledgements

The authors wish to thank G.P. Johari for helpful suggestions and the critical reading of the manuscript.

References

[1] N.O. Birge, S.R. Nagel, Phys. Rev. Lett. 54 (1985) 2674.
[2] K.L. Ngai, R.W. Rendell, Phys. Rev. B41 (1990) 754.
[3] J.M. Hutchinson, S. Montserrat, Thermochim. Acta 286 (1996) 263.
[4] G. Van Assche, A. Van Hemelrijck, H. Rahier, G. Van Mele, Thermochim. Acta 286, 268 (1995) 121.
[5] C. Schick, G.W.H. Hohne (Eds.), Temperature Modulated Calorimetry, Special Issue, Thermochim. Acta 304–305 (1998).
[6] M. Cassettari, G. Salvetti, E. Tombari, S. Veronesi, G.P. Johari, Il Nuovo Cimento 14D (1992) 763.
[7] M. Cassettari, G. Salvetti, E. Tombari, S. Veronesi, G.P. Johari, J. Polym. Sci.: Polym. Physics: Part B 31 (1993) 199.

[8] C. Ferrari, G. Salvetti, E. Tombari, G.P. Johari, Phys. Rev. E 54 (1996) 1058.
[9] C. Ferrari, G. Salvetti, E. Tombari, G.P. Johari, Il Nuovo Cimento D 18 (1996) 1443.
[10] M. Cassettari, F. Papucci, G. Salvetti, E. Tombari, S. Veronesi, G.P. Johari, Rev. Sci. Instrum. 64 (1993) 1076.
[11] D. Bertolini, M. Cassettari, G. Salvetti, E. Tombari, S. Veronesi, Rev. Sci. Instrum. 61 (1990) 2416.
[12] C.J.F. Bottcher, P. Bodewijk, Theory of Electric Polarization, vol. II, 2nd edn., Elsevier, 1978, Ch. 8.
[13] B. Wunderlich, J. Therm. Anal. 48 (1997) 207.
[14] L.C. Thomas, A. Boller, I. Okazaki, B. Wunderlich, Thermochim. Acta 291 (1997) 85.
[15] Akihiko Toda, Tatsuro Oda, Masamichi Hikosaka, Yasuo Saruyama, Thermochim. Acta 293 (1997) 47.
[16] A.A. Lacey, C. Nikolopoulos, M. Reading, J. Therm. Anal. 50 (1997) 279.
[17] J.E.K. Schawe, G.W.H. Hohne, Thermochim. Acta 287 (1996) 213.
[18] D. Bertolini, M. Cassettari, F. Papucci, G. Salvetti Italian Patent No. 9528A/86, CNR, 1986.
[19] M. Cassettari, F. Papucci, G. Salvetti, E. Tombari, S. Veronesi, Italian Patent No. 1252798, CNR, 1991, European Patent Application No. 92830476.5, 1992.
[20] C.A. Taylor, W.H. Rinkenbach, Ind. Eng. Chem. 18 (1926) 676.
[21] M. Reading, Thermochim. Acta 292 (1997) 179.
[22] N.S. Osborne, G. Stimson, D.C. Ginnings, B. of S.J. Res. 23 (1939) 238.
[23] H.L. Finke, M.E. Gross, J. Am. Chem. Soc. 76 (1954) 333.
[24] T.B. Douglas, Ball, D.C. Ginnings, J. Res. Bureau of Standards 46 (1951) 334.
[25] F.S. Omelchenko, Izv. Vyssh. Ucheb. Zaved., Pishch. Tekhnol. 3 (1962) 97.
[26] G. Van Assche, A. Van Hemelrijck, H. Rahier, G. Van Mele, Thermochim. Acta 286 (1996) 209.
[27] E. Tombari, C. Ferrari, G. Salvetti, G.P. Johari, Chem. Phys., 1998, in press.